UC Santa Barbara
UC Santa Barbara Previously Published Works

Title
Dual-reporter SERS-based biomolecular assay with reduced false-positive signals

Permalink
https://escholarship.org/uc/item/05r9t2dq

Journal
Proceedings of the National Academy of Sciences of the United States of America, 114(34)

ISSN
0027-8424

Authors
Chuong, Tracy T
Pallaoro, Alessia
Chaves, Chelsea A
et al.

Publication Date
2017-08-22

DOI
10.1073/pnas.1700317114

Peer reviewed

A dual-reporter SERS-based biomolecular assay with reduced false-positive signals

Tracy T Chuong[a], Alessia Pallaoro[a], Chelsea Chaves[b], Zhe Li[c], Joun Lee[d], Michael Eisenstein[e,f], Galen D. Stucky[a,e], Martin Moskovits[a], and Hyongsok T. Soh[e,f]

Author affiliations

[a] Department of Chemistry & Biochemistry, University of California, Santa Barbara, CA 93106, United States; [b] Department of Chemistry & Biochemistry, Jackson State University, MS 39217, United States; [c] Department of Chemistry & Chemical Engineering, Xiamen University, Xiamen 361005, China; [d] College of Engineering, University of Iowa, Iowa City, IA 52242; [e] Materials Department, University of California, Santa Barbara, CA 93106, United States; [f] Department of Electrical Engineering, Department of Radiology, Stanford University, CA 94305, United States

CATEGORY – APPLIED BIOLOGICAL SCIENCES

ABSTRACT

We present a sensitive and quantitative protein detection assay that can efficiently distinguish between specific and non-specific target binding. Our technique combines dual affinity reagents with surface-enhanced Raman spectroscopy (SERS) and chemometric analysis. We link one Raman reporter-tagged affinity reagent to gold nanoparticles and another to a gold film, such that protein-binding events create a "hot spot" with strong SERS spectra from both Raman reporter molecules. Any signal generated in this context is indicative of recognition by both affinity labels, while signals generated by non-specific binding lack one or the other label, enabling us to efficiently distinguish true from false positives. We show that the number of hot spots per unit area of our substrate offers a quantitative measure of analyte concentration, and demonstrate that this dual label, SERS-linked aptasensor assay can sensitively and selectively detect human α-thrombin in 1% human serum with a limit of detection of 86 pM.

SIGNIFICANCE

While new biomolecular assays are continually being developed to achieve higher detection sensitivities, specificity is often the primary factor limiting an assay's detection threshold—especially in single-label/signal amplification-based assays. This paper describes a novel, sensitive, and quantitative protein detection method that makes use of a dual-reporter approach with enhanced ability to distinguish true positives from false positives. This strategy gives rise to excellent sensitivity and accuracy of measurement, even for low target protein concentrations in complex biological samples.

KEYWORDS

Surface-enhanced Raman spectroscopy (SERS) | protein detection | nanoparticle | ELISA

INTRODUCTION

The enzyme-linked immunosorbent assay (ELISA) remains an indispensable tool for detecting specific target molecules in complex biological samples, (1, 2). ELISA's reliability results from the use of two affinity reagents to capture and sandwich the target protein as a requisite for generating a reporter signal, an approach that reduces false-positive signals. This 'sandwich' assay structure has inspired many groups to develop hybrid versions of ELISA that incorporate novel reporting techniques such as PCR, optical detection, and surface-enhanced Raman spectroscopy (SERS) to further improve sensitivity (3–7).

In conventional sandwich assays, the target is captured by one affinity reagent then detected with a second affinity reagent that is linked to a single reporter. The reporter signal is amplified, generating a readout that is proportional to the concentration of target as determined using a previously derived calibration function. When a reporter-linked affinity reagent binds non-specifically to the substrate, however, it gives rise to false positives that are indistinguishable from true protein capture events (8, 9). It is obvious that the use of a single reporter-conjugated affinity reagent would generally produce a greater frequency of false positives than an assay based on two affinity reagents (both labeled with reporters), as a positive report from the former assay cannot be as confidently associated with the binding to a target protein.

In this work, we describe a sandwich-style protein detection assay that uses two Raman reporters, each conjugated with a distinct affinity reagent. This approach is less susceptible to false positives, resulting in a significantly lower limit of detection (LOD) compared to its single-reporter-based analog. To use SERS to detect binding events, we conjugate one affinity reagent to gold nanoparticles (AuNPs) and the other to a gold metal film. The AuNP-Au film sandwich structure formed in the presence of the target molecule becomes a SERS hot spot, generating a strong and unambiguous signal that indicates a true positive (10). One can analyze the SERS signals by using the traditional 'analog' method to correlate the intensity of one Raman reporter to the known protein concentration, thereby developing an intensity versus concentration calibration curve (5, 6, 10, 11). In contrast, we have opted for an improved 'digital' method, in which many SERS spectra are collected in a pre-determined area of the gold surface under computer control, after which true positives can be identified by using a classical least-squares (CLS) approach to measure the number of sites that report significant contributions from both reporters. Sites with no contributions from either reporter are rejected as producing no signal, while sites that indicate only a single reporter are rejected as false positives. In addition to being automated, the digital approach has the added benefit that one can increase the number of sites from which SERS spectra are collected, trading increased assay time for improved sensitivity and/or accuracy as required. Using this 'SERS-linked sandwich assay' approach, we successfully detected human α-thrombin, and show that our dual-tag approach reduces the LOD to 86 pM relative to the 248 pM LOD achieved with a single-tag approach. Additionally, we show that this approach can be employed with an aptamer-antibody pair to detect tumor necrosis factor alpha (TNF-α), demonstrating the general applicability of this technique.

RESULTS AND DISCUSSION

Assay design and analysis

The assay begins with the conjugation of two different affinity reagents, each with its own Raman reporter, to AuNPs and gold film, respectively (Fig. 1A). In principle, this assay can be performed with any affinity reagent that can readily be linked to gold, including aptamers, antibodies, and peptides. For this initial demonstration, we chose a well-characterized thrombin aptamer pair because such pairs can be readily synthesized with an attached thiol group, allowing for easy conjugation to gold surfaces to form self-assembled monolayers, and are selected to bind to their targets with high affinities (12–14). The AuNPs were functionalized with the thrombin-binding aptamer TBA-29, labeled with the 4-nitrobenzenethiol (NBT) Raman reporter, whereas the gold film was functionalized with the thrombin-binding aptamer TBA-15 conjugated to methylene blue (MB) (15, 16). We initially incubated solutions containing various concentrations of the target protein, thrombin, and a non-target protein (albumin) with AuNPs in order to enable target binding. This mixture was then transferred to the gold film; thrombin molecules that have bound to AuNPs will form a sandwich upon binding to the MB-TBA-15 aptamers on the gold surface, generating a hot spot that enhances the SERS signals of the two reporters (Fig. 1A). The sequence of incubation is important as an allosteric effect had been observed by Olmsted *et al.,* where the TBA-15 binding affinity increases when the thrombin is first bound to TBA-29 (17). Quality-control tests were performed on random batches of AuNP probes and films to confirm reproducibility and functionality, as shown in Figure S1.

We collected assay data by rastering a 55 µm × 55 µm area of the gold film under a Raman microscope at 5 µm intervals, producing an 11 × 11 array of spectra totaling 121 SERS spectra per sampled area (Fig. 1A). The spectrum associated with each of the 5-µm^2 areas is produced by one or more hot spots located within the 1-µm^2 area irradiated by the laser (Fig. S1A). Three sets of 121 spectra were collected for each thrombin concentration. The collection of these 363 spectra, each from a different location on the substrate, took 6 min and provided sufficient precision for all samples tested over the 0.1 to 10 nM thrombin concentration range studied. Under these conditions, the entire assay requires just over an hour in total, with 30 minutes required for each of the AuNP capture and gold film binding steps, prior to the 6-minute detection process. Finally, using CLS analysis, the spectra are categorized in terms of whether they result from one, two, or no reporters (Fig. 1B). By selectively looking at results by one or both reporters, we were able to conduct both single- and dual-tag analyses (see below) from the same set of measurements.

By design, neither the smooth gold film nor the AuNPs alone are able to produce strong SERS signals from their respective Raman reporters in the absence of target (Fig. S2A-B). Assuming that a strong SERS signal will only arise from hot spots, we tested two analysis methods. In the analog single-tag method, the intensity of the AuNP-conjugated reporter was measured to be proportional to the concentration of the target. In the dual-tag method, strong SERS signal could indicate one of three possibilities (Fig. S2). First, it could be a false positive arising from AuNP aggregates that form either in solution prior to addition to the gold film or after addition onto the gold surface. Although such aggregates produce strong SERS spectra, these spectra show large contributions from the NBT reporter on the AuNP, since the hot spots are located primarily at the

interstices between adjacent nanoparticles rather than between AuNPs and the gold surface. Second, false positives may arise from nanoscale defects in the film, such as very small clefts in the gold film, which are likely a result of sample handling. These primarily display the SERS spectrum of the MB reporter that was used to tag the gold film surface. Finally, there are true positives arising from protein-mediated binding of AuNPs to the gold film, which produce intense SERS spectra corresponding to both Raman tags. Examples of such SERS spectra, which have notably different contributions from those generated by the two individual tags, are shown in Figure S1B. We used CLS to quantitatively determine the contribution of each individual reporter, making it possible to select only those true-positive signals arising from strong contributions from both reporters.
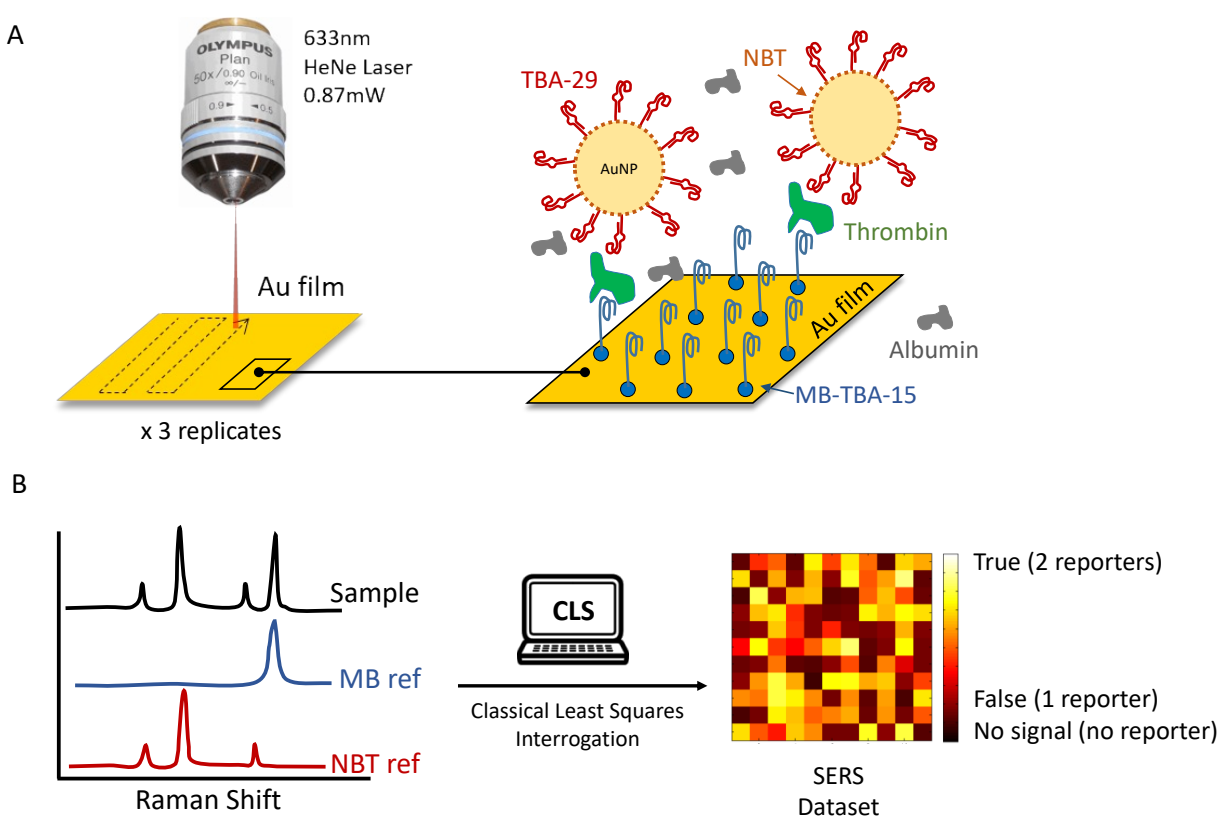

Figure 1. Detection of human α-thrombin. (A) AuNP probes functionalized with TBA-29 and the Raman label NBT capture the target in solutions that contain various concentrations of thrombin and a non-target protein, albumin. These assemblies are in turn captured by a film functionalized with MB-labeled TBA-15 to form SERS hot spots. Spectral data are collected within a designated area of the gold film by raster scanning under a Raman microscope with a 633-nm incident laser. (B) The collection of spectral data per each concentration of thrombin tested is analyzed by classical least-squares (CLS) regression to determine the contribution of each reporter to the spectra and thereby determine true protein-binding events versus false-positives. Physical locations of true- and false-positive binding events are represented in a heat map.

Sensitivity of the SERS assay to changing target concentrations

We examined how SERS signal intensity changes as a function of thrombin concentration, which also helped us to establish the baseline resulting from non-specific binding. We performed assays with known thrombin concentrations (0, 0.1, 0.2, 0.5, 1, 5, 10 nM) in a buffered salt solution containing 5 µM bovine serum albumin, equivalent to the albumin concentration found in 1% human serum. Figure 2A illustrates the relative increase of the 1337 cm^{-1} SERS peak (the NO_2 stretching vibration) produced by NBT-conjugated AuNPs in the absence (left) or presence (right) of thrombin. Scanning electron micrographs (SEM) of the same areas (Fig. 2B, Fig. S4) confirm the increased number of AuNPs bound to the film in the presence of thrombin. A major advantage of the SERS assay is that non-specific binding of particles is very rare in our system due to the electrostatic repulsion by the dense layer of oligonucleotides on the Au surface. The assay proved to be sensitive over a wide range of target molecule concentrations, and measurable SERS signals were observed even from smaller numbers of AuNPs on the film, confirming that the assay is sensitive at low target concentrations (Fig. S4).

In the absence of thrombin, very few AuNPs bound to the Au surface compared to samples containing thrombin, indicating very low levels of non-specific binding. Those few particles primarily consisted of AuNP aggregates, whereas the vast majority of AuNPs remained dispersed in samples with thrombin (Fig. 2B). This important feature can help distinguish true from false positives in the CLS analytical process. Although heat map and micrograph analysis are helpful as a rough visual assessment of target binding at moderate or high concentrations of thrombin, the modest background NBT SERS signal observed in the absence of thrombin (Fig. 2A) limits detection capabilities at low thrombin concentrations, highlighting the primary drawback of single-reporter assays. This limitation is greatly ameliorated by quantitatively determining each of the two reporters' relative contribution to each spectrum using CLS regression. This presents a systematic breakdown of the signal composition, revealing the underlying configuration of the hot spot that produces such a spectrum. This allows us to locate signals produced by aggregate outliers, and reveals that intense spectra in samples without thrombin primarily arise from a single reporter.
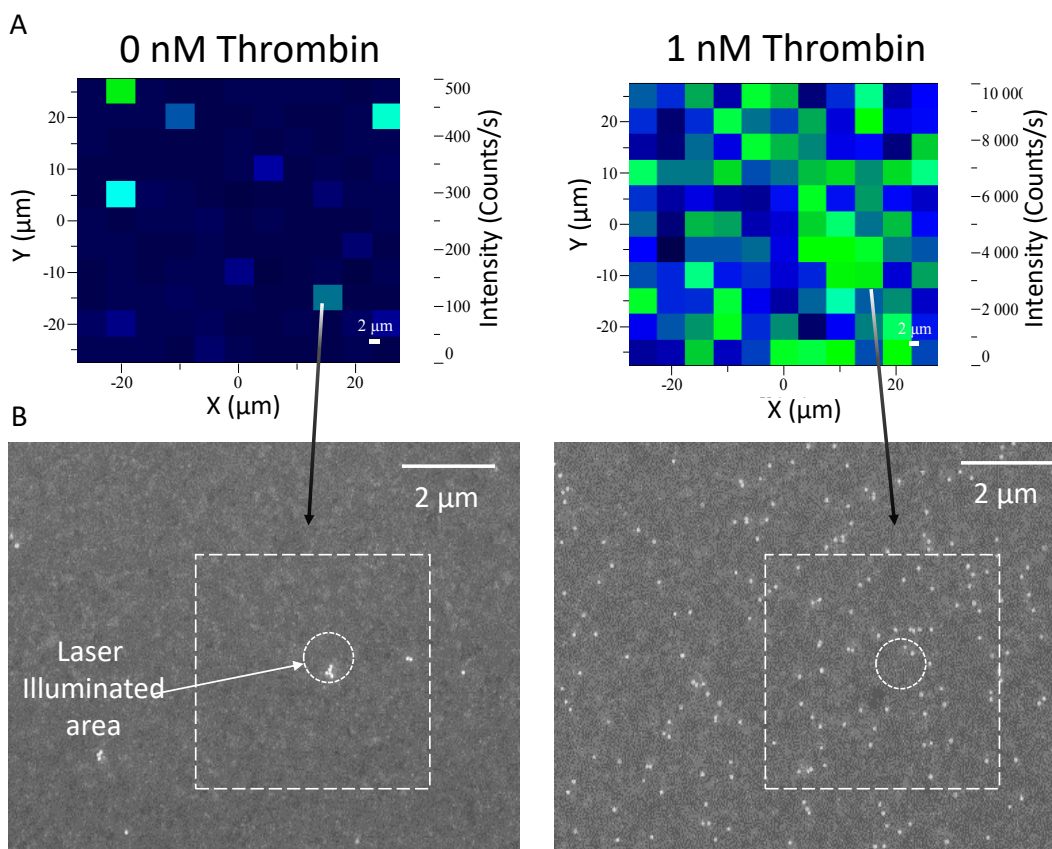
Figure 2. (A) False-color heat map of the intensity of the 1337 cm^{-1} band, indicating SERS hot spots measured for (left) 0 nM and (right) 1 nM thrombin solution. Maximum intensity for each map is (left) 500 counts/s and (right) 10,000 counts/s. The different scale ranges are indicative of the assay's sensitivity to thrombin. (B) Scanning electron micrographs of the same samples.

Identification of false-positives and creation of a calibration curve from true-positive results

For CLS analysis, we fit a linear combination of the individual SERS spectra of the two reporter molecules (Fig. 3A, top, middle) plus an error residual to correct for spectra showing minimal SERS features obtained from the raster scans (Fig. 3A, bottom). Details of the data processing are specified in the Supplementary Information. The bottom panel of Figure 3A shows a representative spectrum from a single rastered spot, 1 of 363 total spectra measured for the 0.5-nM thrombin sample. Careful examination of the peaks in the combined spectrum reveal a slight difference in the ratio of major to minor peak heights shown in the reference spectra (Fig 3A,B). While both tags have major peaks with distinct Raman shifts, some of the minor peaks are common to both reporters. This means that when both molecules are enhanced together, the intensity of these overlapping peaks is summed and may therefore differ relative to the minor peak intensities observed in the SERS spectra from the individual reporters. The magnitudes of the two coefficients returned by the CLS analysis for each rastered spot are assumed to be proportional to the relative contribution of each tag at that location. In cases where the spectra showed very weak or no SERS

6

signals, CLS returned low contributions for the two reporters and high residual values due to poor fit. These data were categorized as blanks. In the coefficient heat map shown in Figure 3B, those locations are given the darkest color. The signals detected were divided into three categories depending on the reporter contributions present in the recorded spectra. AuNP aggregates non-specifically bound to the surface of the gold film in the absence of target produce a SERS signal dominated by NBT. Likewise, surface defects in the gold film produce signals that are dominated by the SERS spectrum of MB. In contrast, SERS hot spots created by protein binding tend to be more evenly spaced across the surface of the film and produce spectra with relatively equal contributions from both MB and NBT (Fig. S4). Spectra containing both Raman reporters with a signal-to-noise ratio equal to or exceeding 3:1 were counted as true positives. We constructed a calibration curve by plotting the percent of true positives of a scanned region versus the known thrombin concentration (Fig. 4A). The calibration curve is monotonic relative to thrombin concentration; although the curve is linear at low concentrations, this linearity is lost at higher concentrations (>1 nM). This is because at low thrombin concentrations, most of the 1 μm^2 illuminated areas reporting true positives contain a single AuNP, whereas at higher concentrations a single laser spot is likely to illuminate several AuNPs at once, such that the assay is no longer "digital". The remaining spectra containing either one of the two tags can either be ignored, or further analyzed to determine the source of the non-specifically produced signals. We would like to emphasize that no background subtraction was required, due to the inherently ultra-low non-specific binding of our system, which represents a major advantage of our methodology.
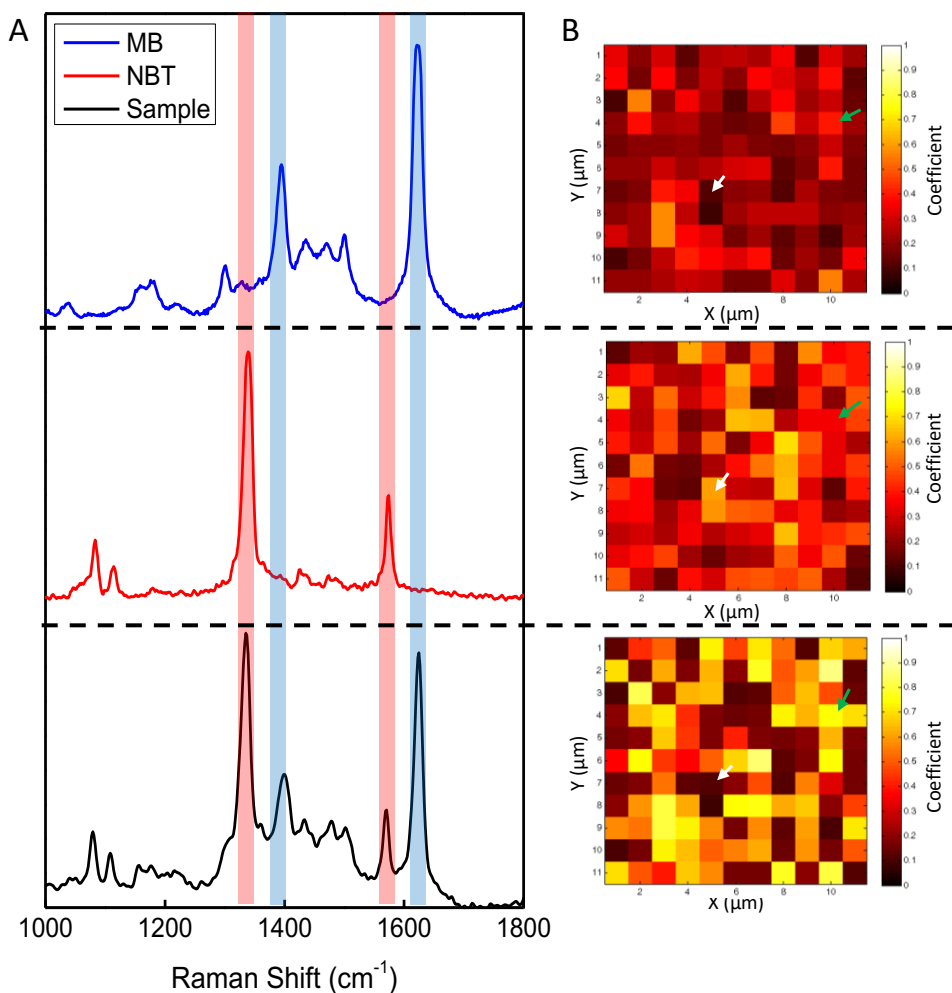
Figure 3. Graphical summary of the results of the CLS analysis used to determine the relative contributions of the two Raman tags for a representative assay with 0.5-M thrombin. (A) SERS spectra in the range from 1,000 to 1,800 cm^{-1}, showing reference SERS spectra of (top) MB, (middle) NBT, and (bottom) a single representative spectrum from the raster scans after an assay has been conducted. The red and blue shaded bars highlight prominent peaks associated with NBT and MB, respectively. (B) Heat maps based on the coefficients returned by CLS analysis for (top) MB, (middle) NBT, and (bottom) the sum of the NBT and MB coefficients for sites with above-threshold values. Brighter color indicates a greater contribution by that tag. Green arrows indicate an example of a true positive sector, where both reporter coefficients are above threshold. White arrows show an example of a false-positive sector, where one of the two reporters is below threshold.

For samples with no thrombin, we found that an average of 0.6% of spectra contained strong NBT contributions. This represents the false-positive rate derived solely from non-specific binding of AuNP aggregates, as shown in Figure 2A. An additional 0.4% of the spectra exhibited high values for the MB coefficient with sub-threshold contribution from NBT, representing hot spots produced

by defects in the gold film. Thus, a total of 1% of the rastered area produced false-positive signals derived from nonspecific sources. Importantly, only 0.3% of the spectra showed above-threshold contributions from both NBT and MB tags.

Using this approach, we were able to generate a reliable binding curve as a function of thrombin concentration in solution (Fig. 4A), which yielded an LOD of 86 pM (18). The LOD was obtained by taking the signal from a blank sample and adding it to the standard deviation obtained from the signal recorded from the lowest tested sample concentration (100 pM). As shown in Figure 4B, spectra containing only one tag occur with approximately double the frequency of spectra containing two tags, especially at low target concentrations. The frequency of false positives is further validated by the results obtained from analyzing the data from a one-reporter approach. We produced a calibration curve by plotting the average intensity of the 1337 cm^{-1} band corresponding to the NBT-conjugated AuNPs for the 121 collected spectra and triplicates against the known thrombin concentration (Figs. 4C, D). With one-reporter assays, any detectable signal is considered to be produced by a protein capture; from the data shown in Figure 2A, we know this to be a false assumption. In the range of 0-1.0 nM, the SERS intensity increased linearly with thrombin concentration in our one-reporter assay. However, the LOD was calculated to be 248 pM in this scenario, a 2.9-fold decrease in sensitivity relative to the two-reporter assay. This decrease in assay sensitivity can be attributed to the inability of the one-reporter assay to reject false-positive signals, and demonstrates the extent to which non-specific binding in the one-reporter system can confound assay sensitivity.

To demonstrate how the sensitivity can be altered by simply changing parameters, we challenged the assay with 50 pM thrombin, which is below the detection limit of this assay (86 pM). As shown in Figure S5, in a collection of 300 spectra, the total count for a 50 pM sample is indistinguishable from that of a 100 pM sample due to high levels of error. However, upon increasing the number of spectra collected to 1,000 spectra (and thereby increasing the collection time from 5 min to ~17 min), the error decreases, and this makes it possible to confidently distinguish the difference between a 50 pM sample and a 100 pM sample. With 2,000 spectra (collection time of ~33 min), the difference is drastic. An increase in binding is also noted when the assay incubation time is increased. By further increasing the number of sites from which spectra are collected or increasing target incubation time during the assay, one can further improve the sensitivity and resolution of the assay at the expense of greater assay time (19).
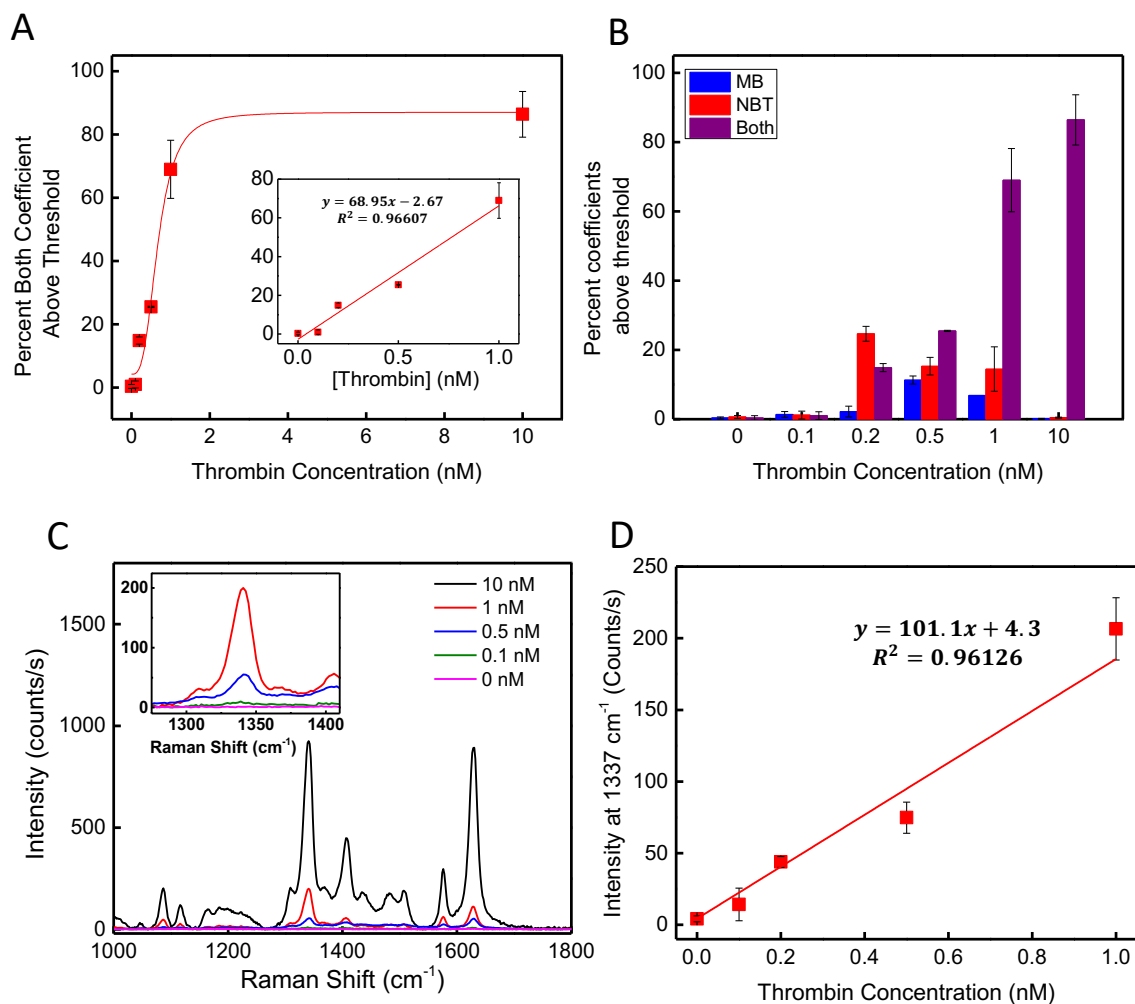
Figure 4. Summary of results from single- and dual-reporter SERS assays. (A) Standard thrombin binding curve in 5 µM albumin for the dual-reporter assay. Inset shows the low-concentration portion of the graph, expanded for clarity. (B) Summary of results from CLS analysis expressed as percent contribution from each tag in the dual-reporter assay. Blue bars (MB only) indicate signal derived from film defects, while red bars (NBT only) indicate spectra derived from AuNP aggregates. Purple bars indicate true protein-binding events. (C) Average intensity of all 121 spectra as a function of thrombin concentration for the single-reporter SERS assay. Inset shows the 1337 cm^{-1} region expanded for clarity. (D) Intensity of the 1337 cm^{-1} peak as a function of thrombin concentration for the single-reporter assay.

Detection in diluted serum

Finally, we investigated how the assay performs in a biologically relevant medium, by testing its capacity to detect thrombin in 1% human serum. Serum is collected by allowing the blood plasma to clot until factors are depleted, after which the clot is removed by centrifugation. Although serum theoretically should be free of clotting factors, trace amounts remain after extraction. To determine how much endogenous thrombin is in the sample, we obtained a reference value using a commercial dual-antibody ELISA kit, with which we determined the concentration to be 183±4

pM. When we analyzed the same sample using the one-reporter approach, we observed a low-intensity NBT signal, but this was indistinguishable from noise. This observation is unsurprising, given that the measured concentration is below the assay's LOD of 248 pM. Using the two-reporter approach, we determined the concentration to be 111±24 pM after testing seven individually prepared samples, which is within the range reported by the ELISA.

Detection of tumor necrosis factor - alpha.
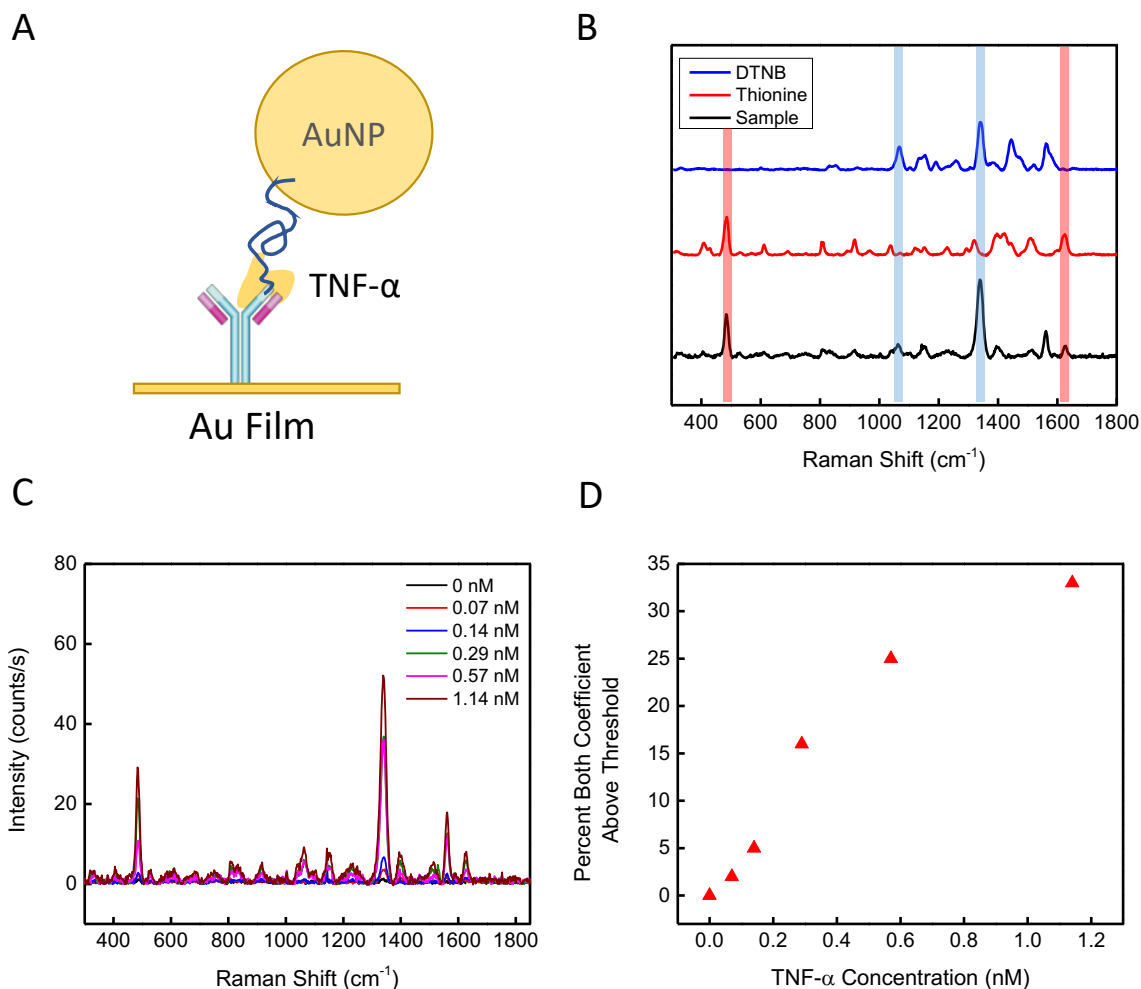
Figure 5. Detection of TNF-α using an antibody-aptamer reagent pair (A) Schematic of the TNF-α detection system, in which labeled antibodies are immobilized on the AuNP film and TNF-α aptamers (blue line) are immobilized on AuNPs. (B) The AuNPs and gold films were respectively labeled with the Raman tags thionine and DTNB. (C) As the concentration of TNF-α protein increases in the solution, an increase in Raman intensity of both labels is observed. (D) Standard TNF-α binding curve in a background of 5 µM albumin.

We chose to use aptamers in this initial demonstration of the SERS assay for their robustness, ease of chemical modification, and cost-effectiveness, but our assay design can also be used with other affinity reagents. We performed a proof of concept assay with a commercially available aptamer-antibody pair for tumor necrosis factor alpha (TNF-α) (Fig. 5A). We used the same procedure described above to prepare AuNPs functionalized with a TNF-α aptamer and thionine as Raman label. For the gold film, we used 5,5′-dithiobis(2-nitrobenzoic acid) (DTNB), a Raman label with a carboxylic acid functional group, to label the anti-TNF-α antibodies (Fig. 5B). As with the thrombin assay, the SERS signal intensity changes as a function of TNF-α concentration with equally sparse non-specific binding (Fig. 5C). We performed assays with known TNF-α concentrations (0, 0.07, 0.14, 0.29, 0.57, 1.14 nM) in a buffered salt solution containing 5 μM bovine serum albumin. As before, we obtained a total of three replicates of 121 spectra to produce a standard curve of true TNF-α binding events. We observed that binding increases monotonically relative to TNF-α concentrations (Figure 5D), and thereby demonstrated the ease with which our assay could be applied to other targets.

CONCLUSIONS

We describe a sensitive, specific method for quantitative target detection that combines the ELISA dual affinity reagent sandwich architecture with SERS. The SERS-based technique utilizes a pair of affinity reagents, each labeled with a Raman reporter; one is conjugated to AuNPs, while the other is bound to a gold surface. The simultaneous binding of the protein to the two affinity reagents produces a SERS hot spot for each binding event. The data are analyzed by using CLS analysis to quantify the results and eliminate false positives. In an initial demonstration with thrombin as a target, we achieved a LOD of 86 pM, and we further show that our assay can be applied to other targets, such as TNF-α. CLS analysis of these spots made it possible to distinguish true-positive SERS spectra produced by both reporters from false-positives produced by only a single reporter. In this initial iteration our thrombin assay delivered a LOD that was higher than that of ELISA (4 pM), which we attribute primarily to the fact that ELISA has an amplification step (through HRP) where as our method is a direct-readout of a single particle binding event. However, our method is capable of detecting physiologically relevant target concentrations in complex mixtures and has a powerful capability to distinguish between true- and false-binding. Furthermore, our assay is considerably faster than ELISA, and we have demonstrated a four-fold shorter assay time in this work. This is because it requires fewer washing steps and, as noted above, is less prone to non-specific binding. Finally, we have demonstrated that higher sensitivity can be obtained by either increasing incubation time to induce more AuNP-target complexes to bind, and thereby shifting the monotonic region towards the lower concentration, or by increasing the area interrogated in order to reduce the deviation. This produces a lower LOD while still resulting in a faster assay than ELISA with the capacity to discriminate between true- and false-binding. In this way, we anticipate that future iterations of our assay will deliver both greater speed and higher sensitivity.

Materials and Methods

<u>Materials</u>

AuNP assembly: All reagents were purchased from Sigma Aldrich and used as received except where specified. For nanoparticle assembly, we used bis(p-sulfonatophenyl)phenylphosphine dihydratedipotassium salt (phosphine ligand, 99%); tris(2-carboxyethyl)phosphine hydrochloride (TCEP, 500 mM); 4-nitrobenzenethiol (NBT, 80%); 6-mercapto-1-hexanol (MCH, 99%); 3,7-diamino-5-phenothiazinium acetate **(**thionine, dye content >85%); 60 nm citrate-capped gold nanoparticles (AuNPs, 2.6×10^{10} particles/mL, Ted Pella); methanol; thrombin-binding aptamer (TBA-29, Integrated DNA Technologies), tumor necrosis factor-α binding aptamer (TNF-α aptamer, Integrated DNA Technologies).

Film assembly: We used thrombin-binding aptamer (MBA-TBA-15, Biosearch Technologies); N-(3-dimethylaminopropyl)-N′-ethylcarbodiimide hydrochloride (EDC, 99%); *N*-hydroxysuccinimide (NHS, 97%); 5,5′-dithiobis(2-nitrobenzoic acid) (DTNB, 98%, Molecular Probes); bovine serum albumin (BSA); TNF-α antibody (MAb11, eBioscience); acetone; isopropanol; silicon wafer (University Wafer); 96-well plate (Corning).

Buffers were diluted with ultrapure water at 18.2 MΩ·cm (EMD Millipore). The buffers used include 4-(2-hydroxyethyl)piperazine-1-ethanesulfonic acid (HEPES, 1 M); Tris-EDTA (TE, pH 8.0, Invitrogen); 20x saline sodium citrate buffer (SSC; 3 M NaCl, 300 mM sodium citrate, pH 7.0, Invitrogen); 7.5 M ammonium acetate solution, 1x phosphate buffer saline (PBS, pH 7.0, Invitrogen).

Prepared assay buffer (50 mM Trizma, 140 mM sodium chloride, 100 mM potassium chloride, and 1 mM magnesium chloride; pH 7.2); 50 mM potassium phosphate buffer (KPB); human serum (male, AB type); 2-(N-morpholino)ethanesulfonic acid hydrate (MES, pH 5); human α-thrombin (Haematologic Technologies) and TNF-α (R&D Systems) are diluted in assay buffer.

<u>Oligonucleotide deprotection</u>

All oligonucleotides (Integrated DNA Technologies and Biosearch Technologies) were purchased at the 1 μM scale in lyophilized form. 5' protection groups were remove by reacting with 1 mL 100 mM TCEP in pH 8.0 TE buffer overnight at room temperature (RT), followed by purification through NAP-10 columns (GE Healthcare). The purified oligo solution was concentrated to 250 μM with Amicon Ultra-4 centrifugal filters (EMD Millipore) in TE buffer for long term storage at -20 °C. Prior to AuNP or gold film conjugation, the oligo aliquots were annealed in 10 mM TCEP at 95 ºC for 5 min to reduce potential disulfide bonds and to break up secondary, hydrogen-bonded structures that the aptamers may have adopted during storage. Aptamer sequences are shown below:

Aptamer	Conjugation substrate	Sequence
MB-TBA-15	Gold film	5' S-$(CH_2)_6$-/MB/iSp18/TTTTTG GTT GGT GTG GTT GG -3' iSp18 is a hexa-ethyleneglycol spacer for increasing flexibility and density of aptamer on the gold film (20)
TBA-29	60-nm AuNP	5' S-$(CH_2)_6$-AGT CCG TGG TAG GGC AGG TTG GGG TGA CT-3'
TNF-α	60-nm AuNP	5' S-$(CH_2)_6$-ATC CAG AGT GAC GCA GCATGC TTA AGG GGG GGG CGG GTT AAG GGA GTG GGG AGG GAG CTG GTG TGG ACA CGGTGG CTT AGT -3'

Preparation of aptamer-nanoparticle conjugates

All incubations under rotation were performed at RT on an Eppendorf rotisserie rotator (6 rpm). All centrifugation (Eppendorf minispin) steps were performed at 4300 rcf for 15 min. AuNP concentrations were verified using UV-vis spectroscopy, calculated with absorbance at 540 nm and an extinction coefficient of 3.5×10^{10} L mol^{-1} cm^{-1} (21). The aptamer-AuNP conjugation was conducted as follows:

We performed ligand exchange on purchased citrate-capped AuNPs to stabilize the particles during aptamer immobilization. 1 mL 60 nm AuNPs from Ted Pella stock were centrifuged to remove storage buffer, re-suspended in 1 mL aqueous solution of 0.9 mM phosphine ligand, and rotated overnight. We linked the thiol-conjugated aptamer to AuNPs following a modified protocol based on the procedure described by Zhang *et al.* (22). Briefly, the resulting phosphine-capped AuNPs were concentrated to 2×10^{11} particles/mL (100 µL) by centrifugation, to which we added 3.2 µL (1.2 µL TBA-29 or TNF-α taken from 250 µM stock without dilution and 2 µL of 500 mM TCEP) of the annealed solution to achieve a final aptamer concentration of 3 µM. To encourage DNA binding, the solution pH was adjusted to 3.0 using sodium citrate (final 10 mM NaCit). After 20 min rotation, the pH was neutralized to pH 7.0 with 1 M HEPES buffer to a final concentration of 130 mM HEPES. To maximize the quantity of aptamer bound to the surface, the particles were salt-aged by adding 20x SSC in 300 mM increments every 20 min to a final NaCl concentration of ~1 M. Along with the first 300 mM SSC addition, we added 50 mM KPB to help the aptamers form G-quadruplex structures and minimize over-packing (15, 23). The AuNPs were sonicated in a bath (Branson Ultrasonic Bath) as needed to prevent aggregation. Finally, the AuNPs were put on the rotator to age overnight in the salt solution. We used Raman label (NBT for thrombin experiments and thionine for TNF-α experiments) and MCH to label and passivate, respectively, the remaining, uncoated Au surface. This was done by adding NBT in methanol (1 mM stock) and MCH (1 mM stock) in ethanol simultaneously to the Au colloidal solution to a final concentration of 100 µM and 5 µM, respectively, after which we rotate the solution for 2 h at RT. For TNF-α experiments, we used an identical labeling procedure but using thionine dissolved in water (1 mM stock) rather than NBT in methanol. After 2 hours, the AuNP conjugates were isolated by centrifugation, and washed in KPB three times to ensure complete removal of unbound reagents. Finally, the concentration of particles was adjusted to 350 pM in assay buffer, and this mixture was then used immediately. We noted that aptamers were displaced from the particles over the course of storage (Fig. S3), and particles were therefore prepared fresh for each experiment.

Preparation of MB-TBA-15 modified monolayer Au film

All incubations under rotation were performed at RT on an orbital rotator in a 96 well plate. As with AuNPs, to prevent oligo displacement over storage, aptamer immobilization were therefore prepared fresh for each experiment.

The MB-TBA-15 aptamers were immobilized onto the film through thiol-gold conjugation. Gold films were prepared by electron-beam deposition (Temescal) on a four-inch silicon wafer. The wafer was cleaned (bath sonication in acetone, isopropanol, and water for 3 min each) and ozone/plasma-scrubbed (Novascan) for 3 min. A 30 nm titanium film was deposited as an adhesion layer at the following rates: 0.05 nm/s to 3 nm, and 0.1 nm/s to 30 nm. 300 nm of Au were layered on top of the titanium layer at the following rates: 0.1 nm/s to 10 nm, 0.2 nm/s to 30 nm, and 0.4 nm/s to 300 nm. The wafer was diced using a dicing saw (Advanced Dicing Technologies) into 4×4 mm squares and stored under nitrogen. Immediately prior to use, the Au films were cleaned by sonication in isopropanol for 3 min and UV-ozone treated for 20 min. For every substrate prepared, 50 µL 2 µM MB-TBA-15 were annealed in 10 mM TCEP at 95 ℃ for 10 min. The annealed oligos were added to the cleaned gold substrates in individual 96 well plates. After 10 min of incubation, 1 µL 500 mM sodium citrate, pH 3.0, was added to the well to lower the pH for 20 min, followed by neutralization with 6.6 µL of 1 M HEPES to reach a final concentration of 130 mM. Finally, 57.6 µL 20x SSC was added to the same well to encourage maximum packing of MB-TBA-15 on the gold films, resulting in a final solution concentration of 1 µM MB-TBA-15 and 1.5 M NaCl. The films were salt-aged under these conditions on a covered plate at RT overnight on an orbital rotator. The next morning, the films were washed three times with 300 µL of 50 mM KPB, delivered by pipette, followed by 300 µL of 30 mM NaOH for 3 min to remove non-specifically adhered aptamers. For each wash, substrates were moved to a new well. Finally, the films were washed with water and submerged in assay buffer for 10 min to prime the films for use in the assay.

Preparation of Mab11 modified Au film

For TNF-α detection, the Mab11 films are prepared using the same 4×4 mm diced Au chips described above. After cleaning the Au films by sonication in isopropanol and UV-ozone treatment, the films were immediately submerged in 200 µL of 5 mM DTNB in absolute ethanol in a well on a 96-well plate and reacted overnight. The next day, the films were washed three times with ethanol, followed by two washes in 0.1 M MES buffer, pH 5. 200 µL of freshly prepared EDC and NHS (400 µM and 100 µM respectively in 0.1 M MES buffer) were added to the films to activate the carboxylic acid functional group for 1 h. The films were washed once with 0.1 M MES buffer, after which 100 µL of 5 µg/mL MAb11 in PBS was added to each film and incubated for 2 h. The substrates were washed with PBS three times. Finally, to block uncoated regions of the gold film, 200 µL of 1% BSA in PBS were added and stored for at least 12 h at 4 ℃ for use the following day.

Protein sandwich assay

The modified AuNPs were added to solutions containing 0, 0.1, 0.2, 0.5, 1, 5, 10 nM thrombin (or 0, 0.07, 0.14, 0.29, 0.57, 1.14 nM TNF-α) as well as either 5 µM albumin in assay buffer or 1% human serum to a final colloidal concentration of 50 pM and a final volume of 100 µL. The solution was mixed for 30 min at RT on an orbital rotator to allow the AuNPs to capture the target in solution. The 100 µL modified AuNP and protein mixtures were added to the gold films in fresh wells and incubated on an orbital shaker at RT for 30 min. After three washes with assay buffer, followed by two washes with KPB to remove unbound molecules, the films were quickly

submerged in 300 mM ammonium acetate to remove excess salts that may hinder microscopic imaging. The film was dried under a nitrogen stream. Raman data were collected as described below, followed by SEM imaging.

Obtaining reference spectra

Reference spectra shown in Figure 3A were obtained by adding 1 μM Raman tag to 100 μL of 100 pM AuNPs after the phosphine ligand exchange step. The particles were incubated for 1 h, after which the tagged particles were dropcasted onto a clean gold film and allowed to dry. Reference SERS spectra were obtained by measuring the AuNP aggregates at the 'coffee-ring' edges.

SERS measurements

SERS measurements were performed on a LabRam Aramis system (Horiba Jobin-Yvon) equipped with a CCD detector thermoelectrically cooled to -70 °C. The sample was excited with the 633 nm HeNe laser (Melles Griot) through a 50x objective lens with 600-μm hole, 400-μm slit width and a 600 lines/mm grating. The laser beam spot size was roughly 1 μm^2, with 0.87 mW laser irradiation power. The exposure was set to 1 s per spot.

Scanning electron microscopy

Electron micrographs were obtained from representative Au film post assay and SERS measurement on a FEI XL40 Sirion FEG digital scanning microscope. Images were taken using 10.0 kV voltage at 10,000x magnification using ultra high resolution.

Thrombin ELISA

The thrombin ELISA (Abnova, KA0511) was performed per manufacturer instructions on 1% human serum to determine the concentration of endogenous thrombin in the sample. Briefly, a 50 μL thrombin standard was prepared at 20 ng/mL. A two-fold serial dilution was performed using the provided EIA dilution buffer to obtain a total of seven standard points (20 ng/mL - 0.313 ng/mL) and a blank containing only the EIA dilution buffer. 50 μL of the standards, seven individually prepared 1% human serum samples, and 5 μM albumin (negative control) were added to the provided 96-well plate and allowed to incubate for 2 h at RT. After washing the wells five times with a wash buffer, 50 μL of biotinylated thrombin antibody was added per well and incubated for 1 h. The wells were washed five times before 50 μL of a SP-conjugate was added per well and incubated for 30 min. The wells were again washed five times before adding 50 μL of chromogen substrate per well and incubated for 10 min. Finally, the chromogenic reaction was stopped using a stop solution. The wells were read at 450 nm immediately afterward, using the TECAN Infinite m 1000. The data was fitted with a four-parameter logistic curve fit per manufacture suggestion.

Statistical/data analysis

We used classical least-squares analysis from the PLS_toolbox software (Eigenvector Research Inc.), accessed within the MATLAB computational environment, to analyze the spectral data. NBT and MB reference spectra were used to construct the model. Reference spectra were baselined and normalized by area within the software, resulting in a model that was used to assess spectra for relative contributions of the two reporters.

## Acknowledgements

Author contributions

Author contributions: T.T.C, A.P., Z.L., J.L., H.T.S., M.M. designed research; T.T.C., C.C., Z.L. performed research; H.T.S., M.M., G.D.S., contributed equally. T.T.C., A.P., H.T.S., M.M. analyzed the data; and T.T.C., M.E, H.T.S., M.M., G.D.S. wrote the paper. The authors declare no conflict of interest.

To whom correspondence should be addressed. Email: moskovits@chem.ucsb.edu, tsoh@stanford.edu, or stucky@chem.ucsb.edu

A

B

Non-specific SERS from aggregation/defects

SERS from protein-mediated binding
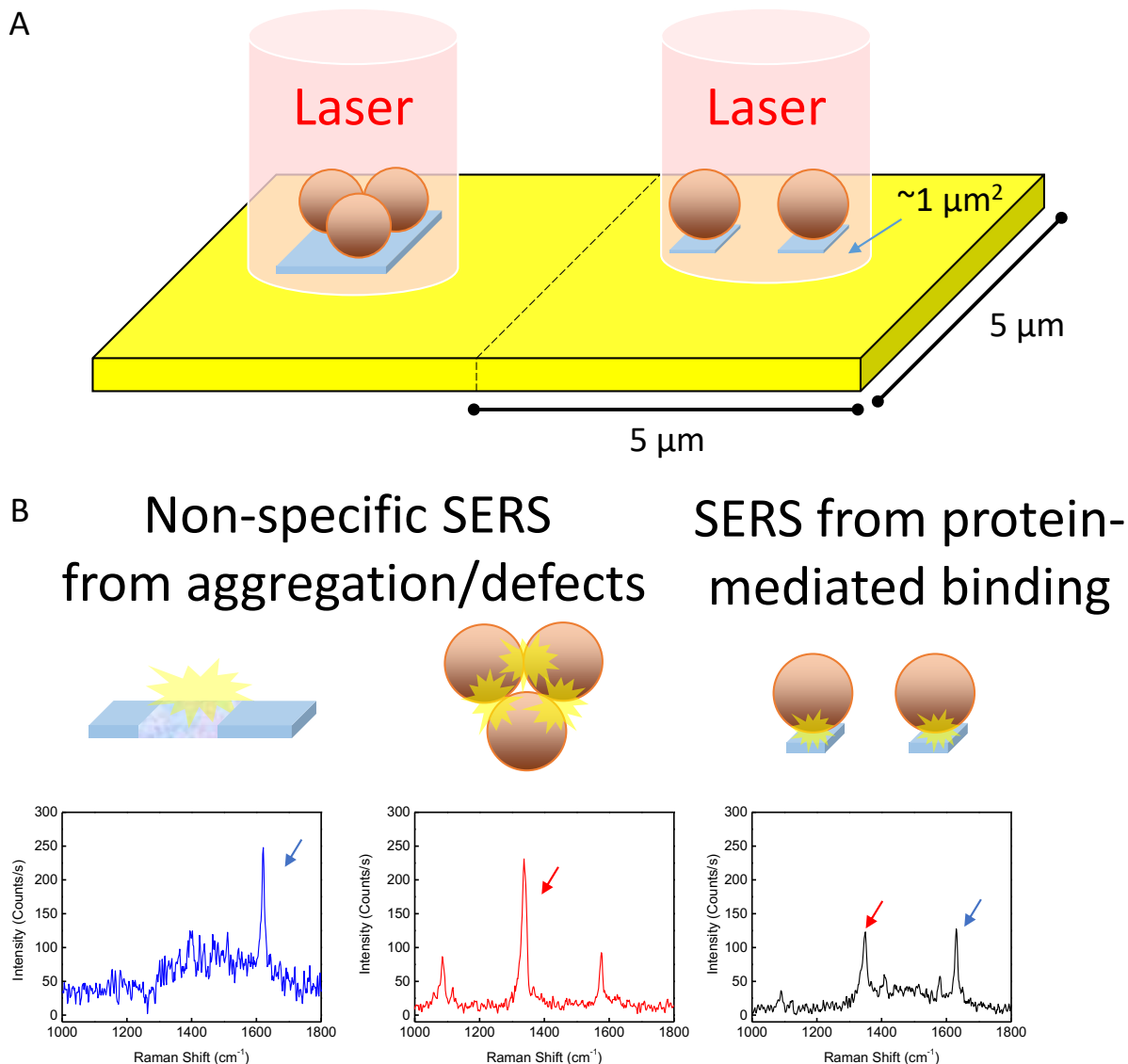

Figure S1. Potential sources of SERS hotspots. (A) The center of each 5 μm^2 area is interrogated by a 1-μm^2 focused laser beam. (B) Three types of hot spots are possible in the assay. (Left) False-positives originating from defects in the film, which are dominated by the MB Raman label, with a strong peak at 1630 cm^{-1}. (Middle) False-positives from AuNP aggregates, which are dominated by the NBT Raman label with a strong peak at 1337 cm^{-1}. (Right) True-positive protein-mediated binding is indicated by near-equal enhancement of MB and NBT peaks.
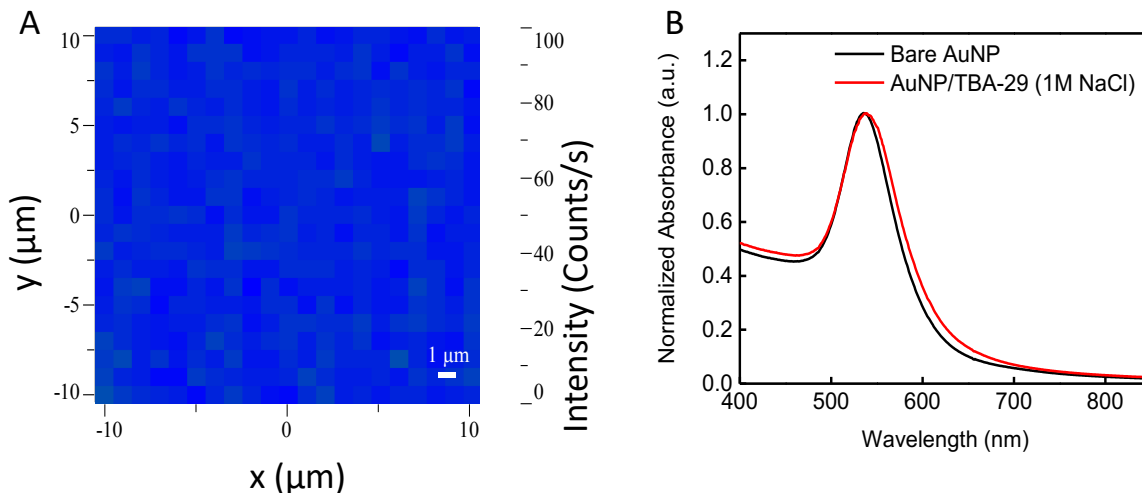
Figure S2. Au film and AuNPs were randomly inspected for quality control. (A) Heat map of gold film with a monolayer of MB-TBA-15. Pristine Au films have barely detectable (less than 30 counts/s) MB signal (1630 cm^{-1}) when excited by the 633 nm laser. The low intensity peaks arise from both the MB molecule and the gold film in resonance with the 633 nm laser. (B) UV-visible spectroscopy of AuNPs before and after TBA-29 and NBT functionalization. When functionalization is performed properly, a slight peak shift to 542 nm is observed due to the new oligo shell on the AuNP. No significant absorbance is observed at 700 nm (indication of unstable/aggregated particles) of functionalized particles in 1 M NaCl.
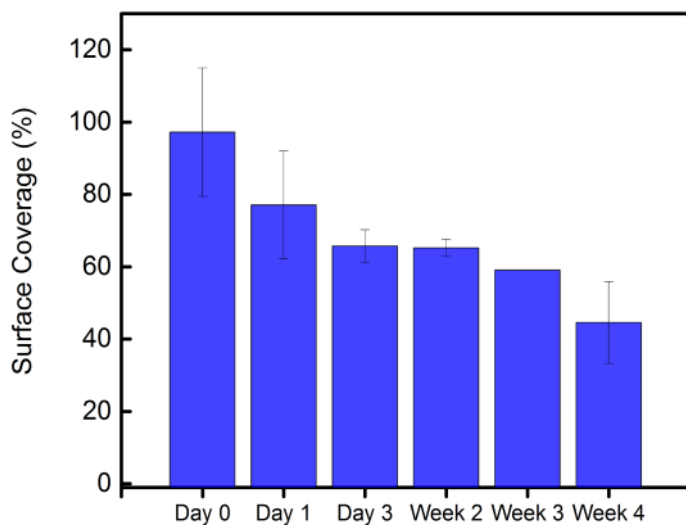

Figure S3. Percent coverage of TBA-29 aptamer on 60 nm AuNPs as a function of time. When particles are freshly functionalized with TBA-29 and NBT, there is an average of 1,830 ± 335 TBA-29 strands per particle. The theoretical maximum coverage is approximately 1,880 strands of TBA-29 per 60 nm particle, assuming the footprint of the TBA-29 G-quadruplex to be 3×2 nm^2.

As particles are stored, the coverage decreases from full coverage to around 50% by week 4. For consistency, particles are always made fresh and used immediately for the assay.
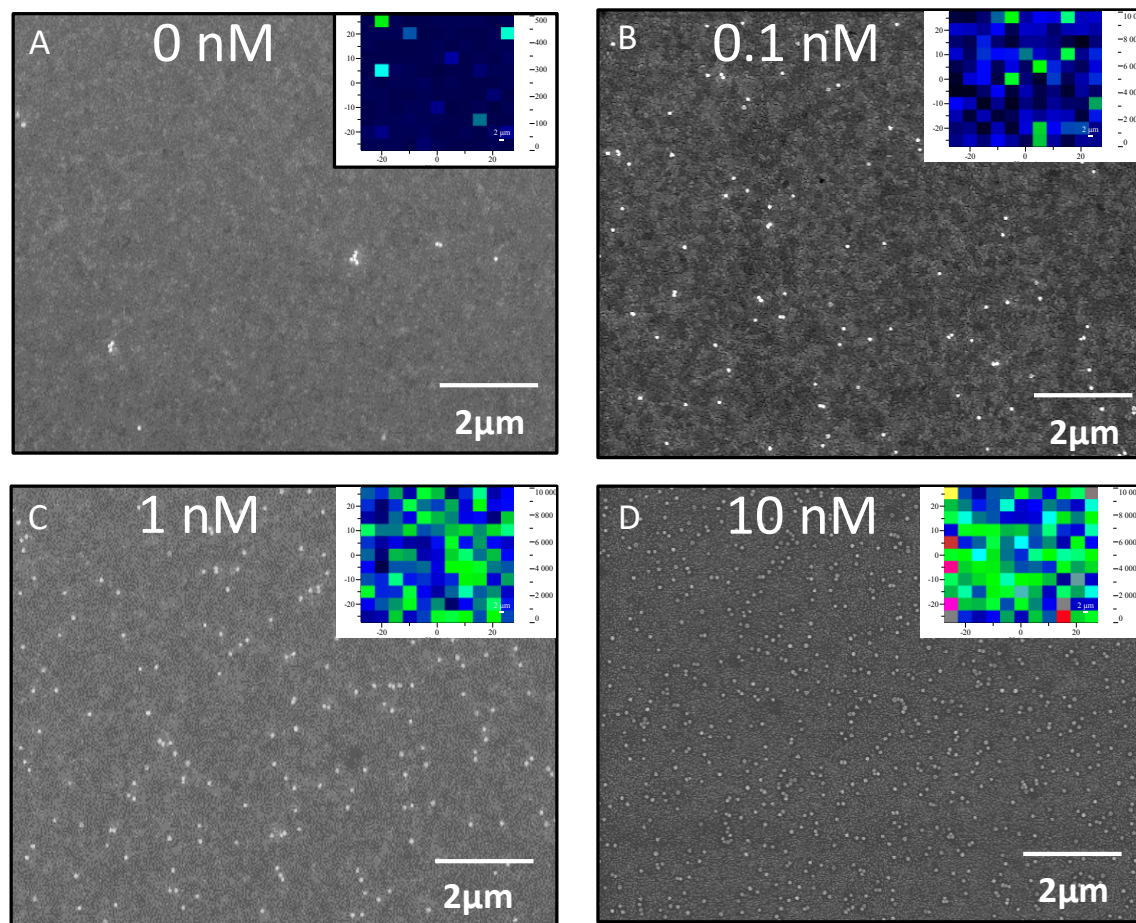
Figure S4. SEM and heat map (insets) of thrombin assays. Maps displaying assay results with 0, 0.1, 1, 10 nM thrombin in buffer. Maximum intensity scale for (A) is 500 counts, while for (B-D) maximum intensity is 10,000 counts, indicating strong SERS with increased protein binding.
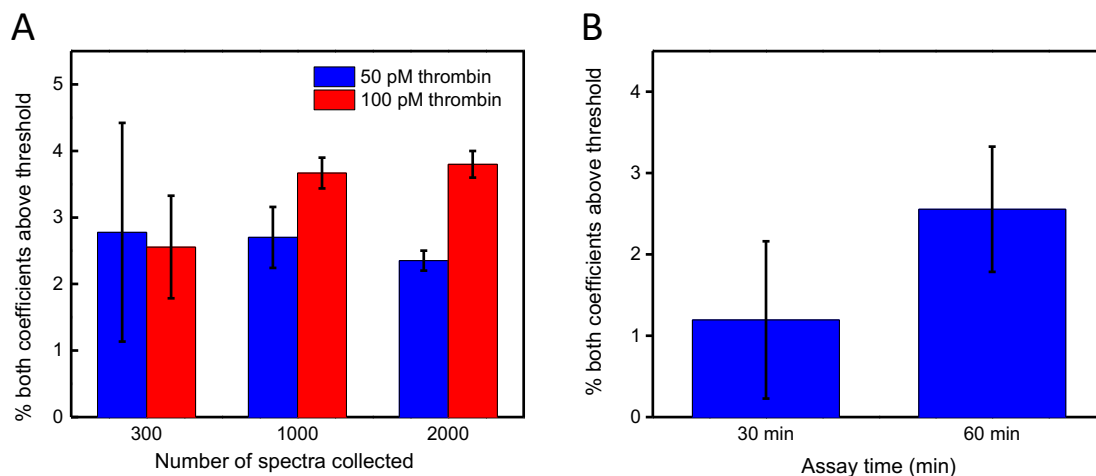
Figure S5. Improving sensitivity by increasing interrogation area or assay time. (A) The error or deviation can be tuned in our assay by simply increasing the number of sites from which spectra are collected. As the number of collected spectra increases, the error decreases and the resolution of the assay improves, resulting in the ability to distinguish 50 pM and 100 pM, at the expense of greater data collection time. (B) If the assay is given greater time to proceed, more particles in solution are bound to the film at lower concentrations. This is demonstrated by performing the assay with 0.1 nM thrombin. By extending the time to allow AuNP-thrombin complex to bind onto the Au film for 60 min rather than 30 min, we observe nearly double the total binding.

Data processing

SERS signals were collected at 5 µm intervals over a 50 µm × 50 µm area on the gold film yielding a total of 121 spectra. Three samples were measured for each thrombin concentration tested. The following thrombin concentrations were tested in a mixture with 5 µM bovine serum albumin: 0, 0.1, 0.2, 0.5, 1, 5, 10 nM. The resulting data were subjected to three types of analysis.

(i) Single reporter analysis

We created a calibration curve that plots the mean intensity of one or more selected Raman bands against the known concentration of the analyte. In our experiments, the 121 individual spectra were averaged, and the intensity of the mean 1337 cm^{-1} band corresponding to the NBT label on the AuNPs was plotted against the known thrombin concentration.

(ii) Dual reporter analysis

The obtained reference spectra and replicates of the 121 SERS spectra from each thrombin sample were normalized over the 1,000-1,800 cm^{-1} spectral range, which includes most of the prominent features associated with MB and NBT (see Methods). CLS analysis determined the values of the two coefficients for each of the two components (MB and NBT), each ranging in value between 0 and 1, which best fit the experimentally measured SERS spectra over the 1,000-1,800 cm^{-1} range,

plus an additional baseline value. We established threshold values for the two coefficients of 0.14 for NBT and 0.2 for MB, reflecting the relative contributions of these two reporters to the overall spectrum, by assessing the minimum values that give rise to a peak signal-to-noise ratio of 3:1. MB has an absorption maximum near 660 nm (24), and upon irradiating the substrate with the 633 nm laser, we observed strong MB fluorescence in the spectra even in the absence of target. To avoid counting this natural fluorescence as true MB reporting, we set the MB threshold higher to 0.2, at which point we no longer observed false-positive contributions from MB.

The data were then separated into three categories: (i) neither reporter above threshold (zero); (ii) only one reporter above threshold (false positive); (iii) both reporters above threshold (true positive). The total number of spectra in each category wasdetermined, and the fraction of spectra above threshold was correlated with the known thrombin concentration.

(iii) Reporter coefficient heat map

To visualize the separation of the coefficients in the scanned area, as in Figure 3B, we replotted the coefficients determined from the two-reporter analysis according to their location coordinates. The top panel of Figure 3 represents the coefficient of NBT for the 121 scanned sectors, while the middle panel represents the coefficient of MB for the same areas. We used three steps to enhance those pixels in the bottom panel of Figure 3. First, sectors below threshold for both reporters had their coefficients automatically set to 0 to represent no signal. Second, pixels or spectra above threshold for both reporters had their coefficients summed. Finally, pixels with one or the other tag below threshold were represented by the corresponding coefficient that was below threshold. Using this method, we could visually map true binding events. It should be noted that this method was solely used for visualization purposes, and was not used to produce the calibration curve.

(iv) LOD calculation

We computed the LOD for the assay as follows:

$$LOD = LOB + 1.645(SD_{lowest\ concentration\ sample})$$

where LOB (limit of blank) is obtained by

$$LOB = mean_{blank} + 1.645(SD_{blank})$$

In which the average signal of the blank (the sample with 0 nM thrombin) is added to the 5% false negative rate (1.645*SD).

Based on our calibration curve, LOB = 0.059 nM and LOD = 0.0858 nM.

REFERENCES

1. Gervais L, De Rooij N, Delamarche E (2011) Microfluidic chips for point-of-care immunodiagnostics. *Adv Mater* 23(24):H151–H176.

2. Engvall E, Perlmann P (1971) Enzyme-linked immunosorbent assay (ELISA) quantitative assay of immunoglobulin G. *Immunochemistry* 8(9):871–874.

3. de la Rica R, Stevens MM (2012) Plasmonic ELISA for the ultrasensitive detection of disease biomarkers with the naked eye. *Nat Nanotechnol* 7(12):821–824.

4. Tsai C, Robinson PV., Spencer CA, Bertozzi CR (2016) Ultrasensitive antibody detection by agglutination-PCR (ADAP). *ACS Cent Sci* 2(3):139–147.

5. Yoon J, et al. (2013) Highly sensitive detection of thrombin using SERS-based magnetic aptasensors. *Biosens Bioelectron* 47:62–67.

6. Grubisha DS, Lipert RJ, Park HY, Driskell J, Porter MD (2003) Femtomolar detection of prostate-specific antigen: an immunoassay based on surface-enhanced Raman scattering and immunogold labels. *Anal Chem* 75(21):5936–5943.

7. Rissin DM, et al. (2010) Single-molecule enzyme-linked immunosorbent assay detects serum proteins at subfemtomolar concentrations. *Nat Biotechnol* 28(6):595–599.

8. Vogt RV., Phillips DL, Omar Henderson L, Whitfield W, Spierto FW (1987) Quantitative differences among various proteins as blocking agents for ELISA microtiter plates. *J Immunol Methods* 101(1):43–50.

9. Song Y, et al. (2014) Point-of-care technologies for molecular diagnostics using a drop of blood. *Trends Biotechnol* 32(3):132–139.

10. Yang K, Hu Y, Dong N (2016) A novel biosensor based on competitive SERS immunoassay and magnetic separation for accurate and sensitive detection of chloramphenicol. *Biosens Bioelectron* 80:373–377.

11. Baniukevic J, et al. (2013) Magnetic gold nanoparticles in SERS-based sandwich immunoassay for antigen detection by well oriented antibodies. *Biosens Bioelectron* 43(1):281–288.

12. Deng B, et al. (2014) Aptamer binding assays for proteins : The thrombin example — A review. *Anal Chim Acta* 837:1–15.

13. Jayasena SD (1999) Aptamers: An emerging class of molecules that rival antibodies in diagnostics. *Clin Chem* 45(9):1628–1650.

14. Chiu TC, Huang CC (2009) Aptamer-functionalized nano-biosensors. *Sensors* 9(12):10356–10388.

15. Tasset DM, Kubik MF, Steiner W (1997) Oligonucleotide inhibitors of human thrombin that bind distinct epitopes. *J Mol Biol* 272(5):688–98.

16. Bock L, Griffin L, Latham J, Vermaas E, Toole J (1992) Selection of single-stranded DNA molecules that bind and inhibit human thrombin. *Nature* 355(6):565–566.

17.	Olmsted IR, et al. (2011) Measurement of aptamer-protein interactions with back-scattering interferometry. *Anal Chem* 83(23):8867–8870.

18.	Armbruster DA, Pry T (2008) Limit of blank, limit of detection and limit of quantitation. *Clin Biochem Rev* 29 Suppl 1(August):S49-52.

19.	Crawford AC, Skuratovsky A, Porter MD (2016) Sampling error: Impact on the quantitative analysis of nanoparticle-based surface-enhanced Raman scattering immunoassays. *Anal Chem* 88(12):6515–6522.

20.	Balamurugan S, Obubuafo A, Soper SA, McCarley RL, Spivak D a. (2006) Designing highly specific biosensing surfaces using aptamer monolayers on gold. *Langmuir* 22(14):6446–6453.

21.	Mulvaney P (1996) Surface plasmon spectroscopy of nanosized metal particles. *Langmuir* 12(3):788–800.

22.	Zhang X, Servos MR, Liu J (2012) Instantaneous and quantitative functionalization of gold nanoparticles with thiolated DNA using a pH-assisted and surfactant-free route. *J Am Chem Soc* 134(17):7266–7269.

23.	Nagatoishi S, Tanaka Y, Tsumoto K (2007) Circular dichroism spectra demonstrate formation of the thrombin-binding DNA aptamer G-quadruplex under stabilizing-cation-deficient conditions. *Biochem Biophys Res Commun* 352(3):812–817.

24.	Singhal GS, Rabinowitch E (1967) Changes in the absorption spectrum of methylene blue with pH. *J Phys Chem* 71(10):3347–3349.